Accelerated Publications

Structure and Function in Rhodopsin. Cysteines 65 and 316 Are in Proximity in a Rhodopsin Mutant As Indicated by Disulfide Formation and Interactions between Attached Spin Labels†

Ke Yang,[‡,§] David L. Farrens,[‡,||] Christian Altenbach,[⊥] Zohreh T. Farahbakhsh,[⊥] Wayne L. Hubbell,*[,⊥] and H. Gobind Khorana*[,‡]

Departments of Biology and Chemistry, Massachusetts Institute of Technology, Cambridge, Massachusetts 02139, and Jules Stein Eye Institute and Departments of Chemistry and Biochemistry, University of California, Los Angeles, California 90095

Received August 21, 1996; Revised Manuscript Received October 3, 1996[⊗]

ABSTRACT: To probe proximity relationships between different amino acids in the interhelical loops in the cytoplasmic domain of rhodopsin, we are using a general approach in which two cysteine residues are introduced at different locations. Here we report on the characteristics of one such mutant that contains the naturally occuring cysteine 316 near the cytoplasmic end of helix G and a second cysteine at position 65 (H65C), near the cytoplasmic end of helix A. The mutant protein after expression in COS-1 cells and reconstitution with 11-*cis*-retinal can be bound to anti-rhodopsin antibody 1D4-Sepharose at pH 6 in a form that contains the two cysteines in the free sulfhydryl form. In this form, the mutant protein reacts as expected with *N*-ethylmaleimide in the dark at room temperature and can be derivatized with nitroxide spin labels. However, under appropriate conditions, the mutant can be isolated with the cysteines in the disulfide form, which has been characterized by analysis of fragments produced on proteolysis with thermolysin. A study of the interactions between nitroxide spin labels attached to the two cysteine residues in the mutant protein indicates that in the dark state they are within about 10 Å of each other. On illumination the distance between the spin labels increases. Collectively, the above results show that, upon folding of the mutant opsin *in vivo*, cysteines 65 and 316, and by inference, helices A and G, are in proximal locations and move further apart upon photoactivation.

Rhodopsin, the dim light photoreceptor in the rod cell, consists of a single polypeptide chain of 348 amino acids. A secondary structure model for the protein, containing seven transmembrane helices, is shown in Figure 1. Recently, cryoelectron microscopy has provided evidence for the presence of seven helices in bovine and frog rhodopsin (Schertler et al., 1993; Unger & Schertler, 1995; Schertler & Hargrave, 1995). A particular arrangement of the seven helices has also been proposed based on a comparative sequence analysis of G-protein coupled receptors (Baldwin, 1993). While the involvement of the cytoplasmic face of rhodopsin in protein−protein interactions occurring in signal transduction is clear, there is little precise information on the relative topography of the cytoplasmic loops or the nature of conformational changes which occur upon rhodopsin light activation.

Our approach to studying the topology and proximity relationships between amino acids in different cytoplasmic loops has been to introduce cysteine residues as attachment sites for probes. For example, by derivatizing the cysteines with *N*-alkylmaleimides, spin labels, or photoactivatable groups, we have gained significant insights into local structure of the interhelical C-D and E-F loop in the cytoplasmic domain (Resek et al., 1994; Ridge et al., 1995; Farahbakhsh et al., 1995; Altenbach et al., 1996). Site-directed spin-labeling studies have also shown that formation of the Meta II photointermediate is accompanied by conformational changes in the cytoplasmic surface of rhodopsin (Resek et al., 1993; Farahbakhsh et al., 1993, Farahbakhsh et al., 1995; Altenbach et al., 1996; Farrens et al., 1996).

We have now extended these studies to the use of mutants containing two reactive cysteines in the cytoplasmic face. With such mutants, one may probe the local structure by disulfide formation and by spin−spin interaction between nitroxide spin labels introduced at the cysteine residues. Here we employ this approach to examine the spatial proximity of the cytoplamic ends of helices A and G in the rhodopsin structure.

In earlier work, it was shown that, of the rhodopsin native cysteine residues, only C140 and C316, both at the cyto-

† This is paper 22 in the series "Structure and Function in Rhodopsin". Paper 21 is by Reeves, Thurmond, and Khorana (1996). This work was supported by NIH Grants GM28289 (H.G.K.) and EY05216 (W.L.H.) and the Jules Stein Professor Endowment (W.L.H.). D.L.F. was the recipient of National Institutes of Health Research Service Award F32 EY06465.

* To whom correspondence should be addressed.

‡ Massachusetts Institute of Technology.

§ Present address: Memorial Sloan-Kettering Cancer Center, 1275 York Ave., New York, NY 10021.

|| Present address: Department of Biochemistry and Molecular Biology, Oregon Health Sciences University, Portland, OR 97201.

⊥ University of California, Los Angeles.

⊗ Abstract published in *Advance ACS Abstracts,* November 1, 1996.

S0006-2960(96)02113-7 CCC: $12.00

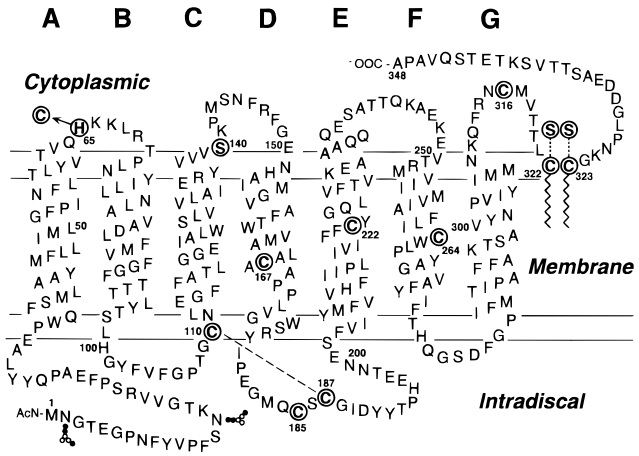

FIGURE 1: A secondary structural model of bovine rhodopsin showing location of cysteines in native rhodopsin as well as sites and designation of cysteine mutants used in this work. The naturally occurring cysteines, Cys-110, Cys-167, Cys-185, Cys-187, Cys-222, and Cys-264, are not reactive at room temperature in the dark. Therefore, these were retained in all the mutants. A base mutant was prepared in which Cys-140, Cys-316, Cys-322, and Cys-323 (the palmitoylation sites) were replaced by serines. The mutant designated H65C was prepared by introducing cysteine at position 65 in the base mutant. In the mutant designated C316, this cysteine was retained in the base mutant. Furthermore, two disubstituted cysteine mutants designated (H65C/C316)-I and (H65C/C316)-II were prepared. In the first, Cys-322 and Cys-323 were replaced by serines, while in the second, Cys-322 and Cys-323 were retained and were shown after expression to be palmitoylated to the same levels as a wild-type control.

plasmic surface, are reactive to sulfhydryl reagents under mild conditions (Resek et al., 1993, 1994). In the experiments reported here, C140 is replaced by serine, leaving C316, near the end of helix G, as the only reactive site. It has been shown that a cysteine substituted at His-65, near the cytoplasmic end of helix A, is reactive to sulfhydryl reagents (Resek et al., 1993, 1994). Thus His-65 was selected as the site for introduction of an additional reactive cysteine. The mutant containing reactive cysteines only at 65 and 316 is designated H65C/C316, although it does contain the full complement of the wild-type cysteines except C140.

The results presented below reveal that the cysteines in H65C/C316 were present either as free sulfhydryls or as a disulfide, depending on experimental conditions. When the cysteines were derivatized with nitroxide spin labels, significant spin−spin interaction between the labels was observed. We conclude from these results that in the dark state rhodopsin, cysteine residues at 65 and 316, and, by inference, helices A and G are in proximity with one another. Photoexcitation of the spin labeled rhodopsin resulted in a decrease in the spin−spin interaction, suggesting that these sites move apart upon metarhodopsin II formation.

EXPERIMENTAL PROCEDURES

Materials. These were as in Yang et al. (1996), except for the following: thermolysin was purchased from Calbiochem (San Diego, CA); 5,5′-dithiobis(2-nitrobenzoic acid) (DTNB, Ellman's reagent) was from Sigma (St. Louis, MO). The sulfhydryl-specific spin label **I** [(1-oxy-2,2,5,5-tetramethylpyrrolin-3-yl)methyl methanethiosulfonate; Figure 2] was a generous gift of Kálmán Hideg (University of Pecs,

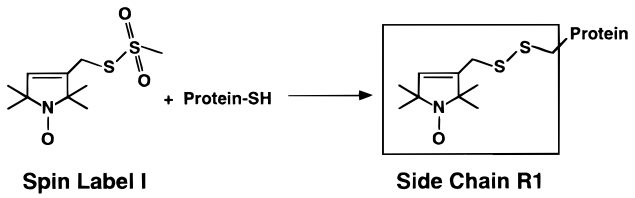

FIGURE 2: Reaction of spin label **I** with a protein sulfhydryl group to generate the nitroxide side chain R1.

Hungary). Bio-Gel P-30 (particle size range of hydrated beads: 90−180 μm) was purchased from Bio-Rad (Hercules, CA).

The buffers used were as follows: Buffer A, 1.8 mM KH_2PO_4, 10 mM Na_2HPO_4 (pH 7.2), 27 mM KCl, 137 mM NaCl, and 1% dodecyl maltoside (DM). This buffer without DM is designated PBS. Buffer B, buffer A + 1 M NaCl, 2 mM ATP, and 2 mM $MgCl_2$. Buffer C, buffer A except that pH was 6 + 1% DM + 1 mM EDTA. Buffer D, buffer C + 1 M NaCl, 2 mM ATP, and 2 mM $MgCl_2$. Buffer E, 20 mM *N*-(2-hydroxyethyl)piperazine-*N*′-2-ethanesulfonic acid (HEPES), pH 7.2 + 0.05% DM. Buffer F, 5 mM 2-(*N*-morpholino)ethanesulfonic acid (MES), pH 6 + 0.05% DM.

Construction of Mutants of the Synthetic Opsin Gene (cf. Yang et al., 1996). H65C/C316 was prepared in two forms from the corresponding mutant opsin genes. In one construct, cysteines 322 and 323, the palmitoylation sites, were replaced by serine. The opsin obtained on expression of this mutant in COS cells is designated (H65C/316C)-I. The second construct, in which the palmitoylation site cysteines 322 and 323 were retained, is designated (H65C/C316)-II. The mutant, (H65C/C316)-I, was constructed by replacement of *Pst*1/*Nhe*1 fragment from the plasmid pH65C with *Pst*1/*Nhe*1 fragment from the plasmid pC316 (Resek et al., 1993), both derivatives of pMT4 containing the synthetic opsin gene (Ferretti et al., 1986). The plasmid p(H65C/C316)-II, in which the two palmitoylation sites, C322 and C323, were retained, was made by replacement of *Pst*1/*Nhe*1 fragment (1925 bp) from the plasmid pH65C with *Pst*1/*Nhe*1 fragment (1925 bp) from pMT4. Large scale preparations of plasmids involved extraction by alkaline SDS and centrifugation to equilibrium in CsCl gradients containing ethidium bromide. The DNA sequences of the mutant plasmids were confirmed by the dideoxy method (Sanger et al., 1977).

Expression and Purification of the Rhodopsin Mutants. The procedures were as described (Yang et al., 1996). The solubilization and purification of the protein were carried out both at pH 6 (buffer C) and at pH 7.2 (buffer A).

Expression of the Rhodopsin Mutant, (H65C/C316)-I, and of the Mutant (H65C/C316)-II in the Presence of [^{3}H]-Palmitic Acid. The cells in three plates ((2−3) × 10^7 cells per plate) (150 × 25 mm) per mutant were incubated at 37 °C with 15 mL of complete medium containing [^{3}H]palmitic acid (50 μCi/mL) after chloroquine treatment during transient transfection. Sixteen hours later, the medium was replaced with fresh 20 mL of the same medium. After additional incubation for 29 h, the cells were washed 3 times with 10 mL of cold PBS (pH 7.2). The rhodopsin mutants were then purified and eluted as before. For determination of the extent of [^{3}H]palmitic acid incorporation, the mutants were purified from excess [^{3}H]palmitic acid by using an SDS−PAGE (10% gel) procedure under nonreducing conditions. The electrophoresis was stopped immediately after the proteins entered

Table 1: Characterization of Rhodopsin Cysteine Mutants

mutant	λ_{max} (nm)	ϵ (M^{-1} cm^{-1})	Meta II decay $T_{1/2}$ (min)[a]	Ellman titration (no. of sulfhydryl groups)[b]	[^{3}H]NEM incorporation[c] (mol/mol of proteins) pH 6[d]	pH 7.2[d]
WT	500	40 600	13.6	2.0 ± 0.2		
H65C[e]	500	41 300	13.3	1.0 ± 0.2		
C316[f]	500	41 000		1.0 ± 0.2		
(H65C/C316)-I	501	42 000	14.7	0.3 ± 0.1	1.96 ± 0.18	0.2 ± 0.1
(H65C/316)-II	499	43 000	12.6			

[a] After purification at pH 7.2. [b] Carried out in the dark at room temperature as in Experimental Procedures. [c] Reaction with [^{3}H]NEM was at pH 6 for 16 h while mutants were bound to 1D4-Sepharose. [^{3}H]NEM was used at 4 mM concentration instead of 1 mM concentration, used in previous work (Ridge et al., 1995). [d] pH at which the proteins were purified. [e] H65C is the mutant with Cys substituted for H65 and Ser subsituted for C140, C322, and C323. [f] C316 is the mutant with Ser substituted for C140, C322, and C323.

the resolving gel, the proteins were visualized by Coomassie staining, and the bands were excised, solubilized in H_2O_2, and then counted for radioactivity (Hames & Rickwood, 1990).

Titration of Sulfhydryl Groups with Ellman's Reagent (DTNB) (Regan et al., 1978). Rhodopsin samples in buffer E were adjusted to a pH between 7.8 and 8.0 by adding 0.5 M K_2HPO_4, pH 11. EDTA was added to a final concentration of 1 mM. DTNB was added to 20-fold excess (from a stock solution in ethanol) to both reference and sample cuvettes, and the time course of the reaction was monitored at 20 °C by absorption at 412 nm for about 10 h.

Digestion with Thermolysin. All manipulations were performed in the dark. A solution of thermolysin in HEPES buffer (20 mM, pH 7.2) was added to 25 pmol (final concentration 0.5 μM) of rhodopsin in buffer E in the presence of 5 mM $CaCl_2$ to a final rhodopsin/thermolysin molar ratio of 5:1 (final volume = 50 μL), and the mixture was incubated for 16 h at 37 °C in the dark. The reaction was stopped by adding EDTA to a final concentration of 10 mM. Electrophoresis was carried out according to Laemmli (1970). For electrophoresis under reducing conditions, DTT was added to a final concentration of 10 mM immediately after the addition of Laemmli buffer, and the samples were then incubated in the dark for 1 h at 20 °C, before SDS−PAGE. For analysis of the thermolysin digests at pH 6, buffer F was used instead of buffer E. After SDS−PAGE, the bands in gels were visualized by silver staining (Wray et al., 1981).

Reactions of H65C/C316-I, 1D4-Sepharose Bound, with [^{3}H]NEM. Prior to use, all buffers were purged with argon at 20 °C for 20 min. Cells (from five 150 × 25 mm plates) containing the rhodopsin mutants were solubilized in 10 mL of buffer C for reaction at pH 6 (or buffer A for reaction at pH 7.2). The mutants were bound to 1D4-Sepharose (150 μL of settled beads) for 3 h at 4 °C in 10 mL of buffer D (or buffer B, pH 7.2). The beads were washed 8 times with a total of 10 mL of buffer F containing 1 mM EDTA (or buffer E, pH 7.2) and were resuspended in 0.5 mL of the same buffer containing 150 mM NaCl. [^{3}H]NEM (0.032 Ci/mmol) was added to a final concentration of 4 mM, and the mixture was nutated at 20 °C in the dark for 16 h. An aliquot (50 μL of settled beads) was thoroughly washed with buffer F (or buffer E, pH 7.2) to remove the excess [^{3}H]NEM. The mutants were eluted with 300 μL of buffer F (or buffer E) containing 100 μM nona-C′-terminal peptide. The eluted samples were then counted for radioactivity.

Reaction of the Cysteine Mutants with the Nitroxide Spin Label **I** *(Figure 2)*. The reaction of the rho-1D4-bound rhodopsin mutants with the spin label (**I**) and elution of the labeled protein from the column were carried out as previously described (Resek et al., 1993).

Reaction of (H65C/C316)-II with NEM in Solution after Reduction with DTT. The mutant (in 100 μL of buffer E) was treated with DTT (2 mM) in the presence of EDTA (1 mM) for 3 h at 4 °C in the dark. To this sample, NaCl (1.5 M) was added to a final concentration of 150 mM, and NEM was then added to a final concentration of 6 mM. The solution was incubated for 16 h at 20 °C in the dark, after which the protein was purified by passage through a Bio-Gel P-30 (200 μL of hydrated beads) spin column. The purified rhodopsin mutant was used for thermolysin digestion and SDS−PAGE.

EPR Spectroscopy. EPR spectra for the spin-labeled mutants at ambient temperature were recorded as previously described (Resek et al., 1993). Low temperature spectra were recorded and fit to a dipole−dipole interaction model to obtain interspin distances as previously described (Farahbakhsh et al., 1995). To estimate the amount of spin label **I** incorporated, the spectra were doubly integrated and compared to the same quantity of a spin standard. The amount of protein was determined from the A_{500}, and the ratio of spins/protein computed from these two quantities.

RESULTS

Characterization of Opsin Cysteine Mutants. All the mutants, expressed in COS-1 cells, were isolated and purified by the standard immunoaffinity method. In general, the yields of the expressed mutants were comparable to that of the wild-type rhodopsin. All the mutants formed rhodopsin-like chromophore with a λ_{max} at or close to 500 nm, and the spectral ratios (A_{280}/A_{500}) were between 1.60 and 1.65. The molar extinction coefficients of the mutants (Table 1) were between 39 900 and 43 000 M^{-1} cm^{-1} compared with 40 600 M^{-1} cm^{-1} for the wild-type rhodopsin. Upon photobleaching, all mutants formed the metarhodopsin II intermediate (λ_{max} = 380 nm). The decay of the latter, as measured by retinal release (Farrens & Khorana, 1995), showed the $t_{1/2}$ for different mutants to range from 12.6 to 14.7 min compared to 13.6 min for the wild-type rhodopsin (Table 1). No major differences were observed in the photobleaching characteristics for the disulfide cross-linked mutants.

Incorporation of [^{3}H]Palmitic Acid during Expression of the Mutant (HC65/C316)-I, (H65C/C316)-II, and WT Opsin. When the above mutants were expressed in COS-1 cells in the presence of [^{3}H]palmitic acid (see Experimental Procedures), analysis showed incorporation of 174 cpm/pmol for wild-type opsin and incorporation of 169 cpm/pmol of

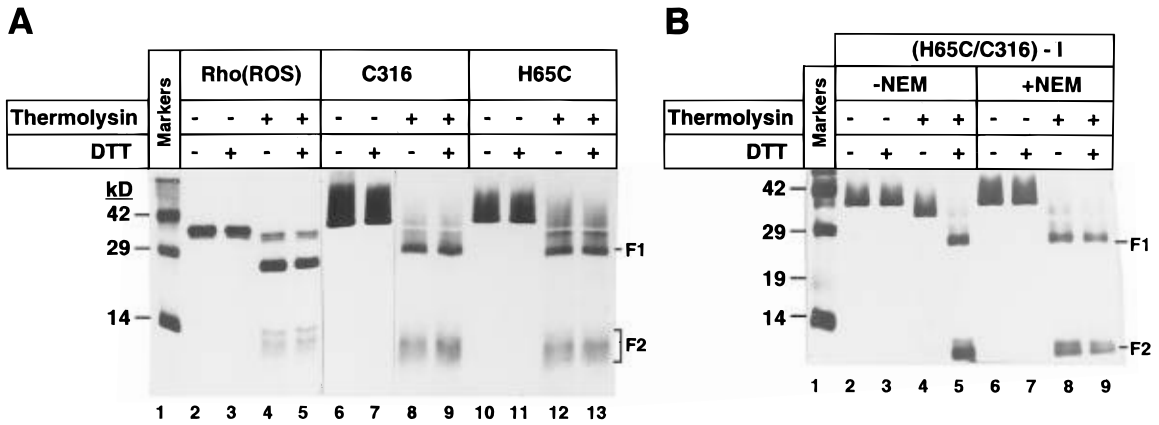

FIGURE 3: SDS−PAGE anaylsis of thermolysin degradation products of rhodopsin and rhodopsin cysteine mutants. (A) Products formed on degradation of WT rhodopsin (ROS), the mutants H65C and C316 under conditions indicated, and in text. (B) Products formed on degradation of the (H65C/C316)-I mutant. The mutant protein was isolated after expression at pH 6.0 or it was alkylated with NEM while bound to rho-1D4-Sepharose beads, as indicated. The results are discussed in text.

(H65C/C316)-II. Under the same conditions, (H65C/C316)-I showed only 10 cpm/pmol of the opsin. Thus, the incorporation of [^{3}H]palmitic acid into wild-type opsin and the mutant (H65C/C316)-II was comparable.

Determination of the Free Sulfhydryl Groups in Cysteine Mutants by Ellman's Reagent. As seen in Table 1, approximately 2 mol of sulfhydryl groups/mol of rhodopsin was observed in the dark in ROS rhodopsin and 1 mole of sulfhydryl group/mol of the rhodopsin mutants H65C and C316; however, only 0.3 mol (in the background range) was found in (H65C/C316)-I when the latter was purified at pH 7.2 (Table 1).

Determination of the Free Sulfhydryl Groups in the Rhodopsin Mutant (H65C/C316)-I by Incorporation of [^{3}H]-NEM. Only 0.2 mol (background level) of a sulfhydryl group/mol of the mutant protein was observed by incorporation of [^{3}H]NEM while the mutant was bound to the 1D4-Sepharose at pH 7.2 (Table 1). However, at pH 6 the mutant bound to 1D4-Sepharose showed an uptake of 2 mol of [^{3}H]-NEM/mol of mutant protein (Table 1). This preparation could also be derivatized with the spin label **I** showing an uptake of 1.7 mol/mol of the protein.

Thermolysin Cleavage of the Cysteine Mutants. The above results on titration with Ellman's reagent as well as derivatization with *N*-ethylmaleimide indicated that the cysteine mutant (H65C/C316)-I prepared at pH 7.2 had undergone disulfide bond formation. To obtain further evidence, proteolysis by thermolysin was studied. Thermolysin is known to cleave bovine rhodopsin mainly at Ser-240 in the cytoplasmic E-F loop and also at two sites (Pro 327/Leu-328 and Lys-339/Thr-340) in the C-terminal sequence (Findlay et al., 1984). Indeed, as seen in Figure 3A, WT rhodopsin (ROS) as well as the mutant H65C (with C316 replaced by serine) and mutant C316 were all degraded under our conditions and formed the expected products. If a disulfide bond between C65 and C316 exists in (H65C/C316)-I, then cleavage at Ser-240 would not release the expected fragments of sizes 26 and about 12 kDa. The results shown in Figure 3B indicate that even when purified and eluted at pH 6, thermolysin-digested (H65C/C316)-I under nonreducing conditions migrated as only one fragment of about 38 kDa size (lane 4). Only in the presence of DTT did this fragment split into the expected smaller fragments (lane 5). Thus, a disulfide bond between H65 and C316

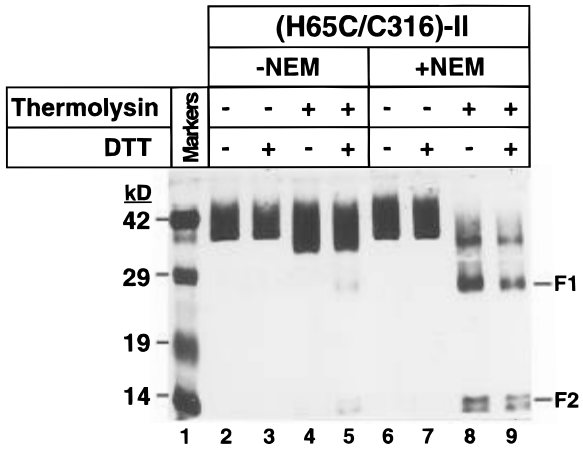

FIGURE 4: SDS−PAGE (15% gel) analysis of thermolysin digests of the double cysteine mutant (H65C/C316)-II purified at pH 7.2. Lane 1, control; lanes 2−5, without NEM treatment; lanes 6−9 with the purified mutant reduced with DTT and alkylated with NEM before thermolysin digestion. Results are discussed in text.

had formed spontaneously. When (H65C/C316)-I was alkylated with NEM while bound to the rho-1D4-Sepharose, then an incorporation of 2 mol of NEM was found (Table 1), and this product on degradation with thermolysin formed the normal fragments (Figure 3B, lanes 8 and 9).

The results of thermolysin treatment of (H65C/C316)-II) are shown in Figure 4. Thus, when the two palmitoyl groups were present in the dicysteine mutant, the 38 kDa product was mainly seen both under nonreducing and reducing conditions (lanes 4 and 5). However, when the sample (H65C/C316)-II was reduced with DTT followed by NEM alkylation of the free sulfhydryl groups before thermolysin treatment, the mutant protein was cleaved into the 26 and 12 kDa fragments (lane 9). Thus, there seems to be a structural constraint in the disulfide bonded (H65C/C316)-II which inhibits normal cleavage by thermolysin at Ser-240.

Spin−Spin Interaction in (H65R1/C316R1)-I. It was found previously (Resek et al., 1993) that mutants H65C and C316 could be labeled quantitatively with spin label **I** to generate the nitroxide side chain R1 (Figure 2) and that the remaining cysteines (Cys-167, -185, -222, and -264) are essentially unreactive to spin label **I** under the spin-labeling conditions employed (contributing less than 30% of the EPR signal in the single cysteine mutants). In the double cysteine mutant,

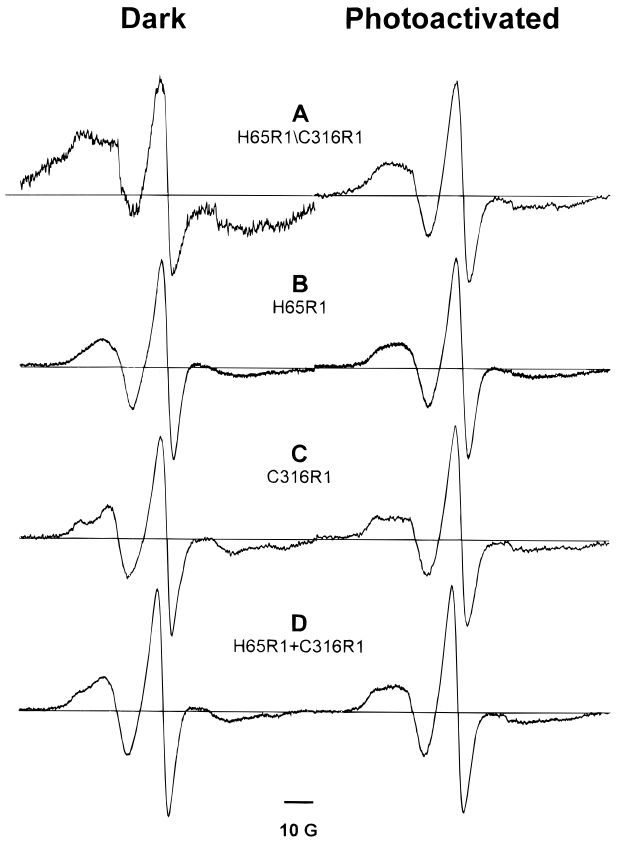

FIGURE 5: Room temperature EPR spectra of the singly and doubly labeled mutants in the dark state (left-hand column) and after photoactivation to produce MII (right-hand column). (A) Spectrum of H65R1/C316R1, the doubly labeled mutant; (B) H65R1, the spectrum of the mutant with a single label at site 65; (C) C316R1, the spectrum of the mutant with a single label at site 316; (D) H65R1+C316R1, the spectral sum of the singly labeled mutants. Differences between the H65R1/C316R1 and H65R1+C316R1 indicate spin−spin interaction.

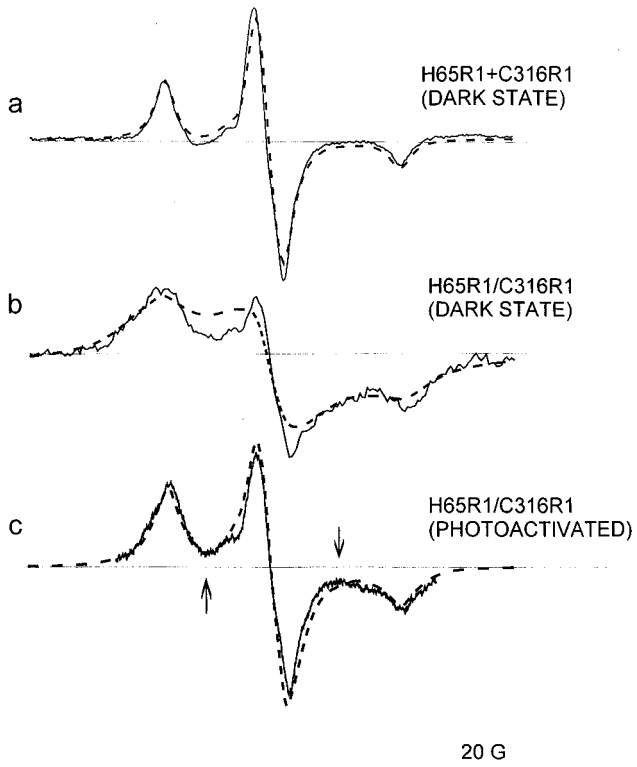

FIGURE 6: Rigid lattice (183 K) EPR spectra for the singly and doubly labeled mutants. (a) Sum of H65R1 and C316R1 (solid line) in the dark state and the simulated powder pattern (dashed line). The principal values of the **g** and **T** tensors used are as follows: $g_{xx} = 2.0082$, $g_{yy} = 2.0059$, $g_{zz} = 2.0027$; $T_{xx} = 5.38$, $T_{yy} = 4.36$, $T_{zz} = 35.2$. (b) Spectrum of the doubly labeled mutant in the dark state (solid line) and the least-squares best fit to a rigid lattice model for dipole−dipole interaction (dashed line). (c) Spectrum of the doubly labeled mutant after photoactivation to produce MII (solid line) and the least-squares best fit to the rigid lattice model (dashed line). For both simulations, the magnetic parameters listed above were used with interspin distance and distance distribution as the only adjustable parameters.

(H65C/C316)-I, 1.7 mol of spin label **I** was incorporated per mole of protein.

Figure 5 shows the EPR spectra recorded at room temperature in both the dark and photoactivated states for the doubly labeled mutant (H65R1/C316R1), the singly labeled mutants H65R1 and C316R1, and the computer sum of H65R1 and C316R1. The spectra for H65R1 and C316R1 in the dark and photoactivated states are consistent with those reported earlier (Resek et al., 1993).

The unique result in the spin labeled mutant H65R1/C316R1 is the unusual breadth (>100 G) of the EPR spectrum in the dark state (Figure 5A, left-hand column) compared to the sum of the single mutants (Figure 5D, left-hand column). This indicates spin−spin interactions between the labels at the two sites. Upon photoactivation, the breadth decreases dramatically, indicating a reduction in the interaction (Figure 5A, right-hand column). The spectra in Figure 5 are scaled in amplitude for convenience of presentation, but when scaled to represent a comparable number of spins, the intensity of the photoactivated spectrum is more than double that for the dark state due to the decrease in width. In fact, the spectrum after photoactivation is rather similar to the sum of the individual spectra from the photoactivated single labeled mutants (compare Figures 5A and 5D, right-hand column).

The spectra were also recorded at low temperature (183 K) to eliminate protein motion, thus allowing the magnitude of the magnetic interactions to be characterized by a rigid lattice model. The spectra of the single mutants H65R1 and C316R1 are essentially identical "powder patterns", both in the dark state and after photoactivation at room temperature before freezing (Figure 6a, solid line). This is expected, since all motion is frozen out and the nitroxides are both solvent exposed (Resek et al., 1993). Simulation of these spectra based on an isotropic distribution of immobile, noninteracting nitroxides is satisfactory (Figure 6a, dashed line). The spectrum of the double mutant in the dark state again reveals distinctive broad spectral features (Figure 6b, solid line). Least-squares fitting of this spectrum to a simple dipolar interaction model yields an approximate interspin distance of 10 ± 3 Å. The fit is not perfect in the region between the low- and mid-field resonance lines. The deviation suggests that there may be a net orientation of the two nitroxides with respect to each other, while the simulation assumes an isotropic distribution of relative orientations. Following photoactivation to the MII state, the strength of the dipolar interaction decreases significantly. That some interaction remains is indicated by the fact that the first derivative intensities do not return to baseline at the positions marked with arrows (compare Figure 6c). The spectrum is best fit with an interspin distance of 15 ± 4 Å.

DISCUSSION

To map proximity relationships between different amino acids in the cytoplasmic loops of rhodopsin, we have taken an approach in which two cysteine residues are introduced at defined positions. The proximity between these cysteine residues is then assessed by a combination of their ability to form disulfide cross-links and the strength of dipolar interaction between nitroxide spin labels attached to the sulfhydryl groups.

In this paper, we report the formation of a disulfide bond between cysteine residues at H65C and C316. This disulfide formation was observed to occur both with or without the presence of the palmitoylation cysteines in the mutant proteins. Both forms of the expressed opsins regenerated with 11-*cis*-retinal in the dark. The non-palmitoylated mutant, (H65C/C316)-I (which was studied in greater detail), could be bound to the 1D-4-Sepharose matrix with the sulfhydryls in their free form. However, after elution from the antibody column, the sulfhydryls in this mutant were no longer available for derivatization, suggesting the presence of a disulfide bond (Table 1). Similarly, mutant (H65C/C316)-II was unreactive toward derivatizing agents after elution from the antibody column.

To obtain further evidence of disulfide bond formation, thermolysin proteolysis and SDS−PAGE analysis was employed. The patterns of the proteolytic fragments from thermolysin-treated WT rhodopsin, mutants C316 and H65C, and the NEM derivatized mutants (H65C/C316)-I and (H65C/C316)-II all gave no evidence of disulfide bond formation (Figure 3). In contrast, after thermolysin cleavage, non-NEM derivatized mutant (H65C/C316)-I showed a single, large fragment on the SDS−PAGE gel, which was split into two fragments upon DTT reduction (Figure 3), indicating the presence of a disulfide bond.

Interestingly, non-NEM derivatized mutant (H65C/C316)-II could not be cleaved by thermolysin. This result shows that the structure with the disulfide bond between H65 and C316 and with the native palmitoyl groups present inhibits the approach of thermolysin to the Ser-240 cleavage site.

Disulfide cross-linking has been previously used to study topology of the bacterial aspartate receptor, and the structural changes associated with signal transduction (Falke & Koshland, 1987; Milligan & Koshland, 1988; Falke et al., 1988). The distance constraint between the α-carbons of cysteines (7 Å) and their orientations for the formation of a disulfide bond are specific (Richardson & Richardson, 1989; Careaga & Falke, 1993). However, it is possible for two cysteines that are farther apart to come together and form a disulfide bond, if there is sufficient flexibility and motion in the region of the protein where the cysteines are located. Thus, we have employed in this study a second complementary approach, nitroxide spin labeling, to investigate proximity between engineered cysteines in rhodopsin. This method has an advantage in providing quantitative information on distances between protein bound spin labels, as well as time-resolved information on structural changes.

The spin−spin interaction between nitroxide side chains in mutant (H65C/C316)-I strongly supports the conclusion reached with chemical cross-linking. The estimated inter-spin distance of ∼10 Å is clearly within the range where cross-linking may be expected (Careaga & Falke, 1992). In addition, results from the dual spin label approach revealed a relative displacement of the two sites by roughly 5 Å upon photoactivation. This movement may be difficult to detect with cross-linking experiments, since the residues are still within cross-linking range for flexible domains (Careaga & Falke, 1992), and the kinetics of the reaction would be a complex function of the sulfhydryl pK_a's, local steric effects, and local pH, all of which may change after photoactivation. However, it must be noted that the absolute value of the estimated distance change may reflect some repacking of the spin label side chain, and the actual displacement of the corresponding α-carbon atoms of the residues may be different.

The change in distance reported here between H65R1 and C316R1 is not unexpected, considering the conformational change detected upon photoactivation at C316R1 in DM solutions (Resek et al., 1993; Figure 5C). The corresponding change in C316R1 mobility was much smaller in the native disk membrane (Farahbakhsh et al., 1993), indicating that the conformational change as seem here is amplified in the detergent micelle.

The proximity of H65 and C316 (and thus their respective helices A and G) is entirely consistent with recent models proposed for packing of the rhodopsin helices (Baldwin, 1993; Schertler et al., 1993). Further, mutational studies have suggested the proximity of helices A and G in the muscarinic acetylcholine receptors (Liu et al., 1995) and the adrenergic receptors (Mizobe et al., 1996).

In conclusion, we have evaluated a double cysteine mutation approach to study the proximity of specific residues in rhodopsin. Disulfide cross-linking and double spin labeling offer two powerful and complementary methods to extract a proximity relationship between cysteines 65 and 316, two residues far removed in primary structure. The result indicates the proximity of the C-terminal domains of helices A and G, and possibly a relative movement of these helices upon photoexcitation. In a forthcoming paper (Farrens et al., 1996), we have extended this strategy to show proximity and movement between helices C and F.

REFERENCES

Altenbach, C., Yang, K., Farrens, D. L., Farahbakhsh, Z. T., Khorana, H. G., & Hubbell, W. L. (1996) *Biochemistry 35*, 12470−12478.

Baldwin, J. M. (1993) *EMBO J. 12*, 1693−1703.

Careaga, C. L., & Falke, J. (1992) *J. Mol. Biol. 226*, 1219−1235.

Falke, J. J., & Koshland, D. E., Jr. (1987) *Science 237*, 1596−1600.

Falke, J. J., Dernburg, A. F., Sternberg, D. A., Zalkin, N., Milligan, D. L., & Koshland, D. E., Jr. (1988) *J. Biol. Chem. 263*, 14850−14858.

Farahbakhsh, Z. T., Hideg, K., & Hubbell, W. L. (1993) *Science 262*, 1416−1419.

Farahbakhsh, Z. T., Ridge, K. D., Khorana, H. G., & Hubbell, W. L. (1995) *Biochemistry 34*, 8812−8819.

Farrens, D. L., & Khorana, H. G. (1995) *J. Biol. Chem. 270*, 5073−5076.

Farrens, D. L., Altenbach, C., Yang, K., Hubbell, W. L., & Khorana, H. G. (1996) *Science* (in press).

Ferretti, L., Karnik, S. S., Khorana, H. G., Nassal, M., & Oprian, D. D. (1986) *Proc. Natl. Acad. Sci. U.S.A. 83*, 599−603.

Findlay, J. B., Barclay, P. L., Brett, M., Davison, M., Pappin, D. J., & Thompson, P. (1984) *Vision Res. 24*, 1301−1308.

Hames, B. D., & Richwood, D. (1990) *Gel Electrophoresis of Proteins*, 2nd ed., p 79, Oxford University Press, Oxford, England.

Laemmli, E. K. (1970) *Nature 227*, 680−685.

Liu, J., Schoneberg, T., van Rhee, M., & Wess, J. (1995) *J. Biol. Chem. 270*, 19532−19539.

Milligan, D. L., & Koshland, D. E., Jr. (1988) *J. Biol. Chem. 263*, 6268−6275.

Mizobe, T., Maze, M., Lam, V., Suryanarayana, S., & Kobilka, B. (1996) *J. Biol. Chem. 271*, 2387−2389.

Reeves, P., Thurmond, R., & Khorana, H. G. (1996) *Proc. Natl. Acad. Sci. U.S.A. 93*, in press.

Regan, C. M., de Grip, W. J., Daemen, F..J., & Bonting, S. L. (1978) *Biochim. Biophys. Acta 537*, 145−152.

Resek, J. F., Farahbakhsh, Z. T., Hubbell, W. L., & Khorana, H. G. (1993) *Biochemistry 32*, 12025−12031.

Resek, J. F., Farrens, D. L., & Khorana, H. G. (1994) *Proc. Natl. Acad. Sci. U.S.A. 91*, 7643−7647.

Richardson, J. S., & Richardson, D. C. (1989) *Prediction of Protein Structure and the Principles of Protein Conformation* (Fasman, G. D., Ed.) pp 1−98, Plenum Press, New York.

Ridge, K. D., Zhang, C., & Khorana, H. G. (1995) *Biochemistry 34*, 8804−8811.

Sanger, F., Nicklen, S., & Coulson, A. R. (1977) *Proc. Natl. Acad. Sci. U.S.A. 74*, 5463−5467.

Schertler, G. F., & Hargrave, P. A. (1995) *Proc. Natl. Acad. Sci. U.S.A. 92*, 11578−11582.

Schertler, G. F., Villa, C., & Henderson, R. (1993) *Nature 362*, 770−772.

Unger, V. M., & Schertler, G. F. (1995) *Biophys. J. 68*, 1776−1786.

Wray, W., Boulikas, T., Wray, V. P., & Hankock, R. (1981) *Anal. Biochem 118*, 197−203.

Yang, K., Farrens, D. L., Hubbell, W. L., & Khorana, H. G. (1996) *Biochemistry 35*, 12464−12469.

BI962113U